Chemical Geology 258 (2009) 269–274

Contents lists available at ScienceDirect

Chemical Geology

journal homepage: www.elsevier.com/locate/chemgeo

Calcite Sm-Nd isochron age of the Shuiyindong Carlin-type gold deposit, Guizhou, China

Wenchao Su [a,b,*], Ruizhong Hu [b], Bin Xia [a], Yong Xia [b], Yuping Liu [b]

[a] Key Laboratory of Marginal Sea Geology, Guangzhou Institute of Geochemistry, Chinese Academy of Sciences, Guangzhou 510640, China
[b] State Key Laboratory of Ore Deposit Geochemistry, Institute of Geochemistry, Chinese Academy of Sciences, Guiyang 550002, China

ARTICLE INFO

Article history:
Received 9 May 2008
Received in revised form 16 October 2008
Accepted 18 October 2008

Editor: D. Rickard

Keywords:
Sm-Nd geochronology
Hydrothermal calcite
Decarbonation and gold deposition
Carlin-type gold deposit
Guizhou

ABSTRACT

Shuiyindong is one of the largest and highest grade, stratabound Carlin-type gold deposits in China. It is hosted in Permian bioclastic limestone near the axis of an anticline. Hydrothermal calcite is common on the periphery of central zones of ferroan carbonate dissolution that provided the main source of iron that was sulfidized during gold deposition. These calcite veins contain relatively high concentrations of rare earth elements with MREE-enriched patterns, and yield Sm-Nd isochron ages of 134±3 Ma to 136±3 Ma, with significant different initial ε_{Nd} values of −12.9 and −2.0, respectively. These ages are interpreted to record age of decarbonation and gold deposition during the late stages of Yanshanian Orogeny. The initial Nd isotopic compositions of the calcites suggest that Nd was primarily derived from the Permian Longtang Formation that hosts all ore bodies at the deposit. This study shows that Sm-Nd isotopic compositions of hydrothermal calcites can be used to constrain the age and source of Nd in Carlin-type gold deposits.

1. Introduction

Sediment-hosted gold deposits, also known as Carlin-type gold deposits, are among the largest hydrothermal gold deposits in the world (Kesler et al., 2005), currently being sought and mined in the United States and China (Tretbar et al., 2000; Hu et al., 2002). They are characterized by decarbonation (carbonate dissolution), argillization, sulfidation, and silicification of typically calcareous sedimentary rocks (Hofstra and Cline, 2000). Gold and pyrite precipitate together from H_2S-rich fluids by sulfidation of dissolved iron from host rocks (Hofstra et al., 1991; Stenger et al., 1998; Hofstra and Cline, 2000; Emsbo et al., 2003; Su et al., 2008).

Direct dating of these deposits has been problematic, complicated by the fine-grained nature of alteration and mineralization, and lack of minerals clearly associated with gold deposition that is suitable for isotopic dating (Tretbar et al., 2000). Most attempts to determine the age of Carlin-type gold deposits have been indirect. Only a few deposits have been dated by $^{40}Ar/^{39}Ar$ on adularia (Groff et al., 1997) and Rb/Sr on galkhaite (Tretbar et al., 2000), involving (U-Th)/He and fission-track dating on apatite (Chakurian et al., 2003) or cross-cutting relationships between dated igneous rocks and mineralization. The paucity of dates for Carlin-type gold deposits in Guizhou hampers understanding of their genesis and relation to the geotectonic evolution of southwest China.

The ideal way to determine the age of gold deposits is to analyze minerals that are known to have formed coevally with the gold (Bell et al., 1989). For Carlin-type gold deposits, numerous studies have shown that gold deposition is closely associated with decarbonation of the host strata and provided the main source of iron for sulfidation during gold deposition (Hofstra et al., 1991; Stenger et al., 1998; Hofstra and Cline, 2000; Emsbo et al., 2003; Su et al., 2008). If we can determine the age of decarbonation, the time of gold mineralization should be closest to the age of decarbonation. Here, we report the first Sm-Nd dates on hydrothermal calcite veins from the periphery of central zones of decarbonation and gold deposition in the Shuiyindong Carlin-type gold deposit in Guizhou, China. These calcite veins contain relatively higher concentrations of rare earth elements (REEs) with MREE enrichment than pre-ore calcite veins and variable Sm/Nd ratios that are suitable for Sm-Nd isotopic dating (Bell et al., 1989; Halliday et al., 1990; Chesley et al., 1991; Darbyshire et al., 1997; Peng et al., 2003a,b).

2. Geological setting

The Shuiyindong mine is located approximately 20 km northwest of the town of Zhenfeng in Guizhou, China, and is one of the largest (more than 100 tonnes Au) and highest grade (7 to 18 ppm), stratabound, Carlin-type gold deposits in China (Fig. 1). The deposit is situated near the axis of the striking Huijiabao anticline and is hosted

* Corresponding author. State Key Laboratory of Ore Deposit Geochemistry, Institute of Geochemistry, Chinese Academy of Sciences, Guiyang 550002, China. Tel.: +86 851 5891359; fax: +86 851 5891664.
E-mail address: suwenchao@vip.gyig.ac.cn (W. Su).

0009-2541/$ – see front matter © 2008 Elsevier B.V. All rights reserved.
doi:10.1016/j.chemgeo.2008.10.030

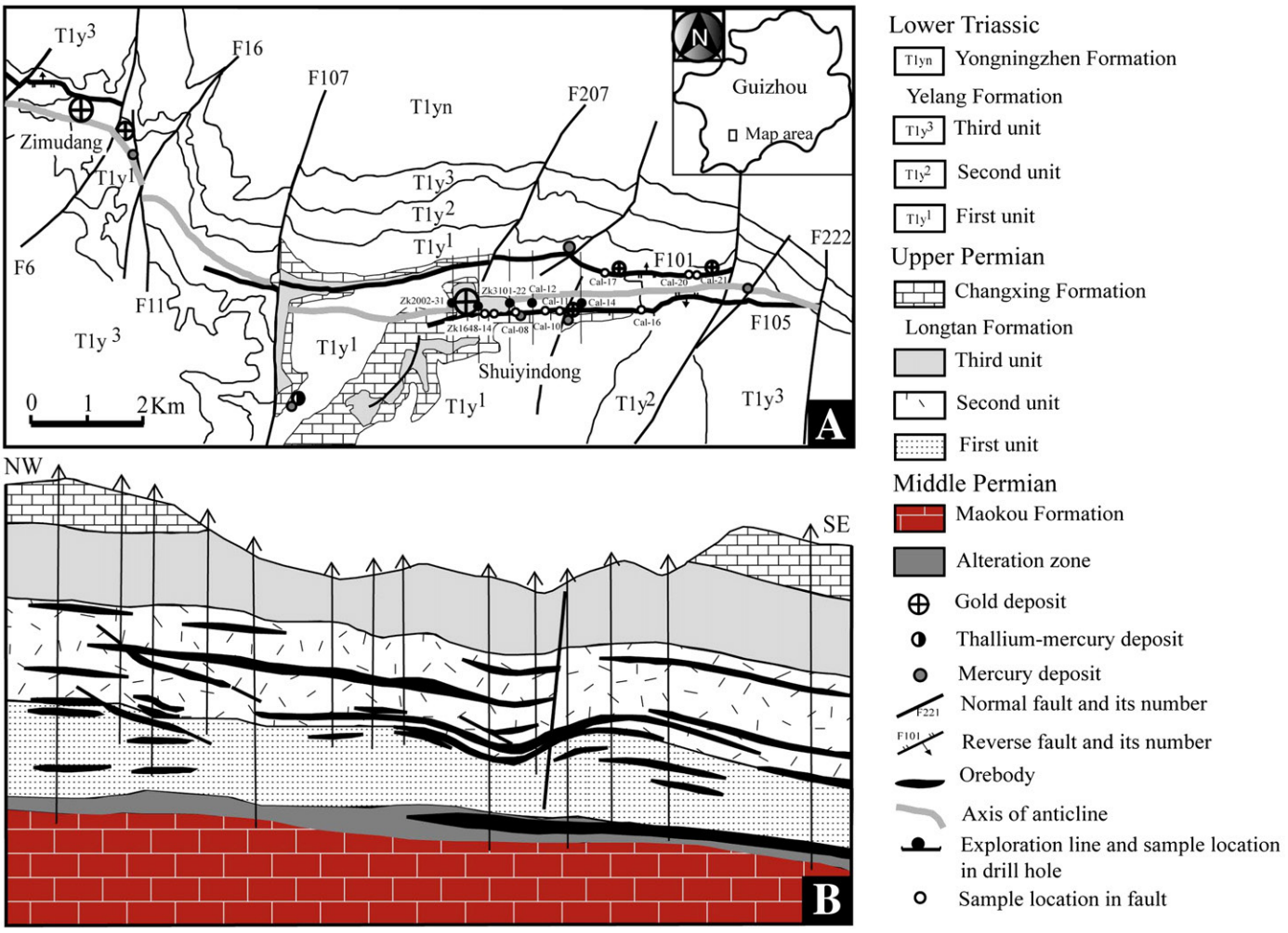

Fig. 1. Geologic plan (A) and cross section (B) of the Shuiyindong Carlin-type gold deposit.

in bioclastic limestone of the Permian Longtan Formation. Geological descriptions of the deposit were given by Su et al. (2008).

Mineralization in the district is hosted by Permian and Triassic strata that consist of tuffaceous bioclastic limestone, siltstone, and argillite. These strata were deformed into a near east-west-trending anticline, with limbs cut by reverse faults F_{101} and F_{105}, respectively. Gold mineralization occurs mainly on the flanks of the anticline and is preferentially disseminated in bioclastic limestone and calcareous siltstone of the first and the second units of the Longtan Formation at depths of 100 to 900 meters below the surface (Fig. 1B). A lower grade ore body is hosted in silicified, brecciated argillite and limestone at the unconformity between the Permian Maokou massive limestone and the first unit of the Longtan Formation, and in reverse faults with small pods of orpiment and realgar. No felsic intrusive rocks of any age have been observed in the vicinity of the deposit. Late Permian alkali flood basalt outcrops in the northwestern part of the district and lamprophyre dykes with an Ar-Ar age of 85 Ma (Su, 2002) occur ca.25 km east of the district.

Gold mineralization is closely associated with decarbonation, silicification, sulfidation and dolomitization, similar to Carlin-type gold deposits in Nevada, USA (Hofstra and Cline, 2000). Decarbonation and silification of limestone are evident from small relict inclusions of ferroan calcite and dolomite in quartz (Fig. 2C–F), which are similar to those of jasperoid quartz (Lovering, 1972). Sulfides observed in the deposit consist mainly of arsenian pyrite, arsenopyrite, marcasite, and lesser orpiment, realgar and stibnite. Small amounts of gold-bearing arsenian pyrite and arsenopyrite are enclosed within Fe-poor dolomite (Fig. 2C and D), whereas a large amount of gold-bearing arsenian pyrite and arsenopyrite are disseminated in jasperoid quartz grains (Fig. 2E) or concentrated along jasperoid quartz grain boundaries (Fig. 2F). Here the dolomite was partially or completely dissolved. Gangue minerals consist of quartz, dolomite, calcite, and clay minerals (e.g. kaolinite), and lesser fluorite. Calcite and dolomite commonly fill fractures on the periphery of zones of decarbonated rocks (Fig. 2A), and locally within such zones in the reverse faults F_{101} and F_{105} (Fig. 2B). Thus, the calcite veins are contemporaneous with gold mineralization or formed thereafter. Petrographic observations (Fig. 2C–F) and covariance of Au, As, Sb, and Sr in the fluids from LA-ICP-MS of fluid inclusions studies suggest that deposition of As-, Sb-sulfides and Au was concurrent with calcite or dolomite crystallization (Su et al., in press). These carbonate veins are believed to have formed where acidic ore fluids were neutralized nearby unexposed gold mineralization (Su et al., 2008), and are used in this study to constrain the age of gold deposition.

3. Sampling and analytical method

Sm and Nd isotope data were obtained from hydrothermal calcite veins along the anticline in the Shuiyindong district (Fig. 1A). Nine calcite veins occur in the reverse faults F_{101} and F_{105} that host small orpiment and realgar bodies with low grade gold mineralization (Fig. 2B). Five calcite veins are from drill cores at depth of 184 to 50 meters below the surface and commonly fill fractures on the periphery of zones of decarbonated rocks (Fig. 2A). Some calcite veins

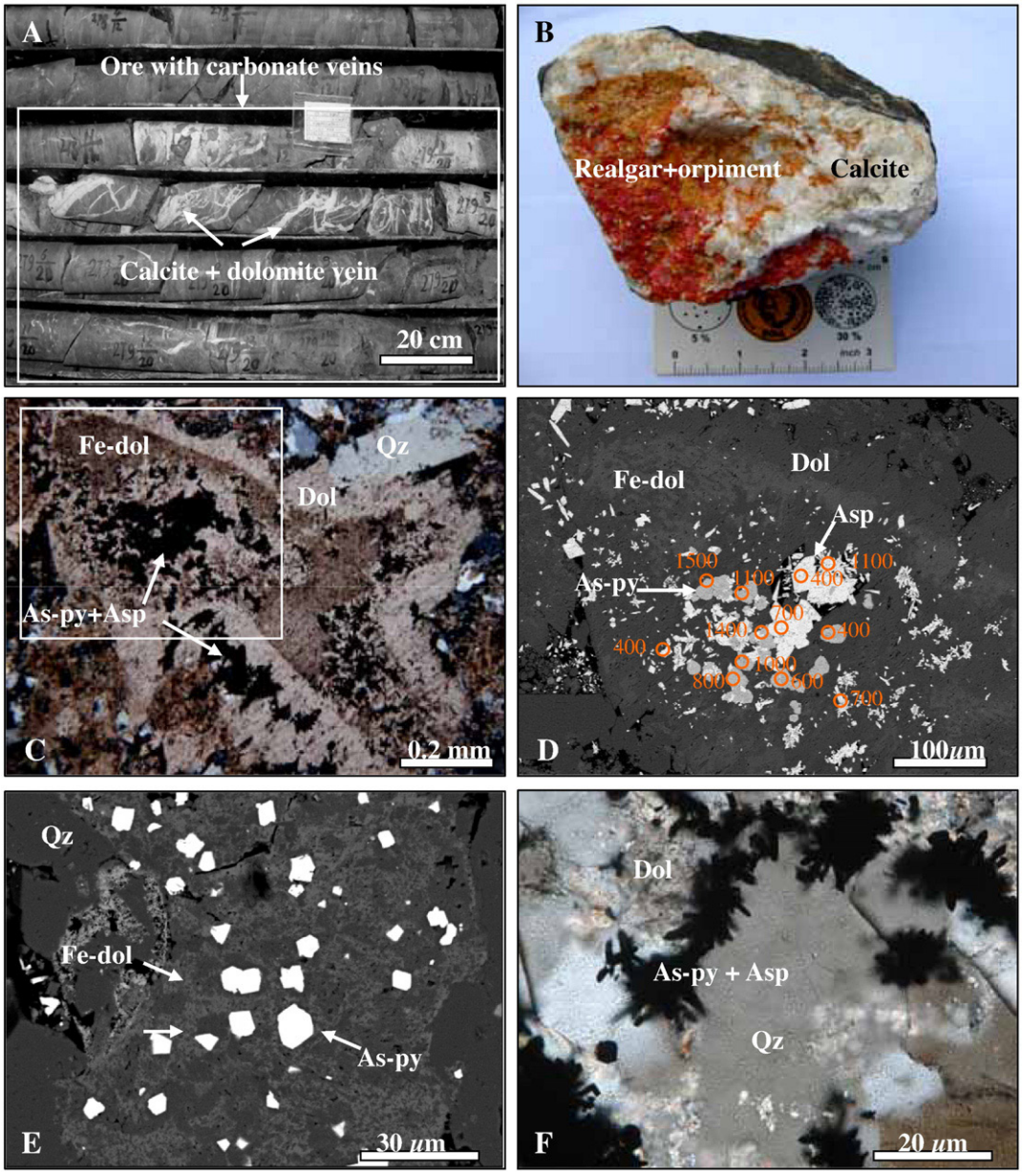

Fig. 2. (A) Example of calcite and dolomite veins from a drill core fill fractures on the periphery of zones of decarbonated rocks. (B) Example of calcite, realgar and orpiment occurs in the fault. (C) Polarized light photomicrograph showing gold-bearing arsenian pyrite and arsenopyrite co-precipitated with Fe-poor dolomite after ferroan dolomite dissolution. (D) EMPA back-scattered electron (BSE) image of inset in (C). The circle and the number denote the spot position of WDS of EMPA and concentration of gold (in ppm), respectively. (E) EMPA back-scattered electron (BSE) image of the gold-bearing arsenian pyrite in jasperoid quartz that contains small relict inclusions of ferroan dolomite. (F) Polarized light photomicrograph showing gold-bearing arsenian pyrite and arsenopyrite concentrated along the jasperoid quartz grain boundaries. Abbreviations: Qz = quartz; As-py = arsenian pyrite, Asp = arsenopyrite; Dol = dolomite; Fe-dol = ferroan dolomite.

contain intergrown realgar and orpiment that are clearly ore-related, based on petrographic observations and poor Fe in gold-bearing fluids in nature (Su et al., in press).

Pure calcite separates were hand-picked under a binocular microscope, and were crushed to 200 mesh in an agate mortar. Prior to isotopic analysis, concentrations of rare earth elements (REEs) in subsamples from the separated calcites were determined by an ELAN 6000 inductively coupled plasma quadrupole mass spectrometer (ICP-MS) at the Guangzhou Institute of Geochemistry, Chinese Academy of Sciences. Calcite for Sm and Nd contents and isotopic compositions analyses were used in the procedure described by Peng et al. (2003b). The samples were dissolved in Teflon vessels with a mixture of HF and $HClO_4$ in a ratio of 10:1 at 150 °C for at least 12 h, until complete decomposition was achieved. Two separated sample aliquots, each weighing 150 mg, were dissolved, one for spiking and determination of Sm and Nd concentrations and the other for the determination of present-day $^{143}Nd/^{144}Nd$ ratios. Separation of Sm and Nd was done by a reverse-phase extraction technique with HDEHP coated on Teflon powder. Sm and Nd concentrations were determined by isotope dilution using ^{149}Sm-^{146}Nd spike solution. Isotopic ratio measurements were made on an IsoProbe T thermal ionization mass spectrometer at Tianjin Institute of Geology and Mineral Resources, CAGS. Nd ratios were normalized to $^{146}Nd/^{144}Nd$ ratio of 0.7219. The reproducibility of the isotopic ratios is better than 0.005% (2σ); the precise for Sm and Nd concentrations is less than 0.5% of the quoted values (2σ). Concentrations for BCR-1 determined during this study were 6.57 ppm for Sm, 28.75 ppm for Nd and 0.512644±5 (2σ, n=6) for $^{143}Nd/^{144}Nd$, consistent with the literature values of 6.58 ppm for Sm, 28.8 ppm for Nd (Bell et al., 1989). Replicate analyses of the Johnson and Mattey® Nd standard (JMC) gave a $^{143}Nd/^{144}Nd$ ratio of 0.511132±5

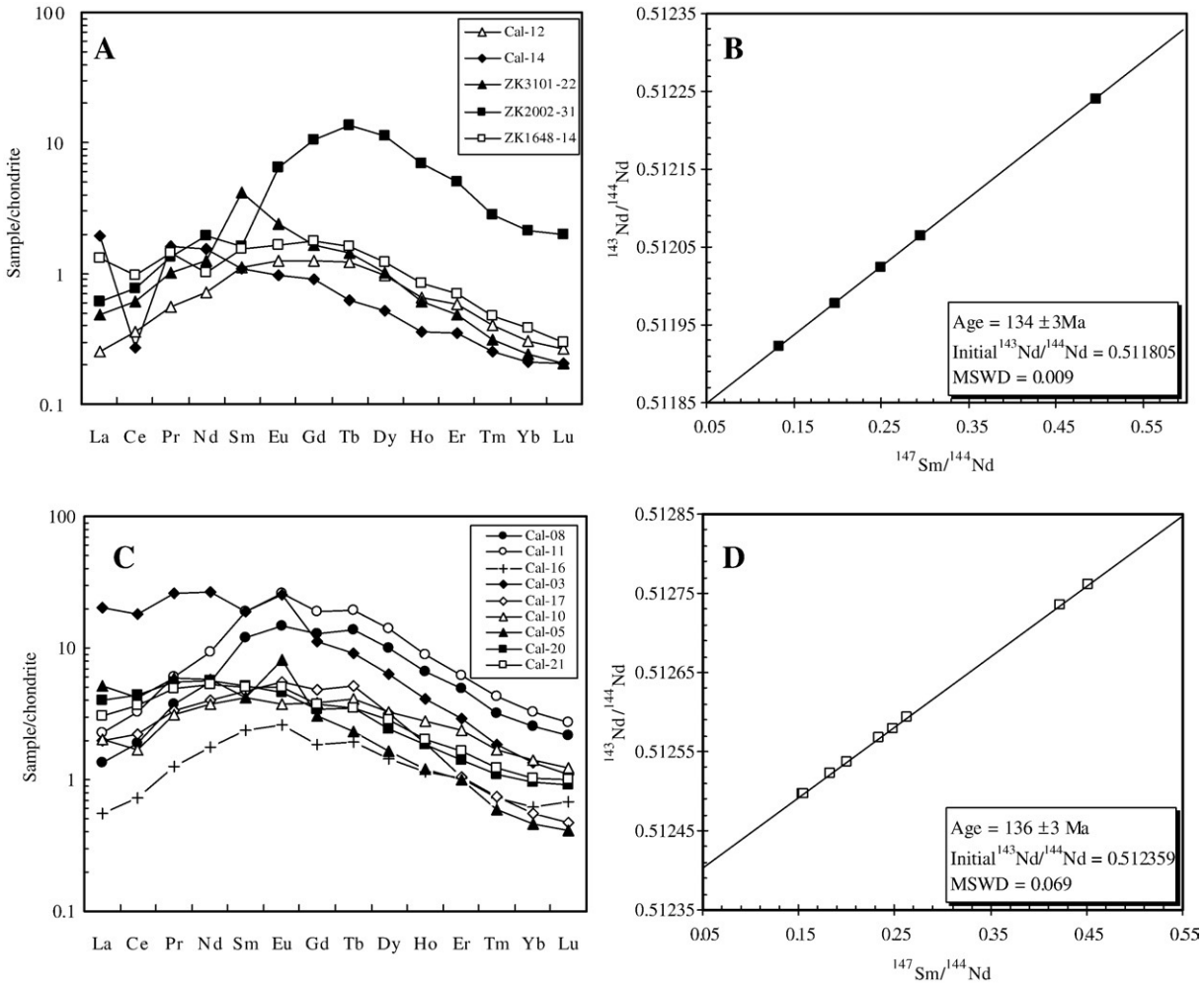

Fig. 3. The chondrite-normalized REE patterns (A and C) and corresponding Sm-Nd isochron ages (B and D) for the calcite veins from the Shuiyindong deposit. All data are normalized using the chondrite REE values of Herrmann (1970).

(2σ, n=6). Blanks during this study averaged 0.03 ng for Sm and 0.05 ng for Nd. The decay constant used in the age calculation is $\lambda^{147}Sm = 6.54 \times 10^{-12}$/yr. The Sm-Nd isochron ages in Fig. 3 were calculated with the ISOPLOT 2.9 computer program (Ludwig, 1996).

4. Result and discussion

Rare earth elements concentrations and isotopic compositions of the calcite veins are presented in Tables 1 and 2, and displayed in Fig. 3, respectively. All calcite veins contain higher concentrations of rare earth elements than pre-ore calcite veins, with the ∑REEs contents in the range of 2.18 to 55.66 ppm. The chondrite-normalized REE patterns for all calcite veins show MREE enrichment (Fig. 3A and C). This characteristic is very similar to those of fluorite veins coeval with gold and antimony mineralization in the Qinglong district reported by Peng et al. (2003a), which is hosted in altered basaltic volcanic tuff that overlies the Permian Maokou limestone in the western part of the Shuiyindong district (Fig. 4). The ore-related calcite veins with MREE

Table 1
Rare earth element data (ppm) for calcite samples from the Shuiyindong deposit

Sample No.	Locality	Occurrence	La	Ce	Pr	Nd	Sm	Eu	Gd	Tb	Dy	Ho	Er	Tm	Yb	Lu
Cal-08	F105	Cc	0.43	1.77	0.45	3.33	2.38	1.08	3.99	0.70	3.07	0.49	1.05	0.10	0.57	0.07
Cal-11	F105	Cc + real	0.73	3.08	0.73	5.58	3.82	1.89	5.85	0.96	4.32	0.65	1.30	0.14	0.72	0.09
Cal-16	F105	Cc	0.18	0.68	0.15	1.05	0.48	0.19	0.57	0.10	0.44	0.08	0.21	0.02	0.14	0.02
Cal-03	F105	Cc	6.54	17.10	3.10	16.06	3.81	1.87	3.46	0.46	1.96	0.30	0.61	0.06	0.29	0.04
Cal-17	F101	Cc	0.63	2.10	0.40	2.40	0.95	0.41	1.51	0.26	1.00	0.14	0.22	0.02	0.12	0.02
Cal-10	F105	Cc	0.64	1.58	0.38	2.26	0.85	0.28	1.20	0.20	1.02	0.20	0.50	0.05	0.31	0.04
Cal-05	F105	Cc	1.66	3.96	0.71	3.50	0.85	0.60	0.95	0.12	0.51	0.09	0.21	0.02	0.10	0.01
Cal-20	F101	Cc + real	1.28	4.18	0.67	3.40	1.04	0.34	1.06	0.18	0.75	0.13	0.30	0.04	0.21	0.03
Cal-21	F101	Cc + real	0.99	3.46	0.59	3.16	1.00	0.37	1.16	0.18	0.89	0.15	0.35	0.04	0.23	0.03
Cal-12	Drill hole ZK5117, 184 meters	Cc + real	0.09	0.32	0.07	0.46	0.22	0.09	0.32	0.06	0.29	0.05	0.12	0.01	0.07	0.01
Cal-14	Drill hole ZK8301, 145 meters	Cc	0.67	0.25	0.20	0.99	0.21	0.07	0.24	0.03	0.16	0.03	0.07	0.01	0.05	0.01
ZK1648-14	Drill hole ZK1648, 104 meters	Cc	0.45	0.89	0.17	0.95	0.30	0.12	0.46	0.08	0.36	0.07	0.14	0.02	0.09	0.01
ZK3101-22	Drill hole ZK3101, 50 meters	Cc	0.17	0.55	0.12	0.81	0.81	0.17	0.43	0.07	0.31	0.05	0.10	0.01	0.05	0.01
ZK2002-31	Drill hole ZK2002, 100 meters	Cc	0.21	0.70	0.16	1.23	0.32	0.47	2.72	0.64	3.37	0.55	1.02	0.09	0.47	0.07

Abbreviations: Cc = calcite, Real = realgar.

Table 2
Sm, Nd and Sr isotope compositions of calcite veins from the Shuiyindong deposit

Sample No.	Sm (ppm)	Nd (ppm)	$^{147}Sm/^{144}Nd$ (atomic)	$^{143}Nd/^{144}Nd$ (2σ) (atomic)	$^{87}Sr/^{86}Sr$ (2σ)
Cal-08	2.3002	3.0752	0.4522	0.512762±6	0.707083±10
Cal-11	3.8689	5.5334	0.4227	0.512735±5	0.707203±21
Cal-16	0.4683	1.0775	0.2628	0.512593±9	0.707482±13
Cal-03	3.6978	14.5286	0.1539	0.512496±7	0.707251±25
Cal-17	0.9178	2.2416	0.2475	0.512579±6	0.707991±11
Cal-10	0.8437	2.1825	0.2337	0.512567±8	0.707217±13
Cal-05	0.8203	3.2117	0.1544	0.512497±8	0.707152±16
Cal-20	0.9776	3.2226	0.1834	0.512523±12	0.707125±13
Cal-21	0.9602	2.8964	0.2004	0.512537±7	0.707143±10
Cal-12	0.2227	0.4570	0.2946	0.512064±6	0.707729±8
Cal-14	0.2044	0.9306	0.1328	0.511922±15	0.707614±10
ZK1648-14	0.2869	0.8801	0.1971	0.511978±20	0.708003±24
ZK3101-22	0.8120	0.9904	0.4957	0.512241±18	0.707610±11
ZK2002-31	0.3900	0.9459	0.2493	0.512024±7	0.706620±18

enrichment are distinct from the regional pre-ore calcite veins with LREE enrichment and negative Eu anomalies, and are used successfully as a pathfinder for exploration of unexposed Carlin-type gold mineralization in the Shuiyindong district.

MREE-enriched patterns have also been recently observed in hydrothermal calcite coeval with antimony mineralization in China (Peng et al., 2003b), and in natural terrestrial waters and acidic leachates (Johannesson and Lyons, 1995; Johannesson et al., 1996) but, currently, is not well understood. Johannesson et al. (1996) proposed solid-liquid exchange reactions, dissolution of MREE-enriched surface Fe-Mn coatings, particulates, and secondary mineral phases, and sulfate complexation as possible mechanisms to develop the MREE-enriched patterns. We cannot eliminate the possibility that mineral inclusions are present in the calcite analyzed. Fluid inclusion studies show that homogenization temperatures for the calcites from the Shuiyindong are about 200–230 °C. Thermodynamic calculations suggest that at elevated temperatures (>250 °C) Eu^{2+} should be dominant over Eu^{3+} (Sverjensky, 1984), and may substitute for Ca^{2+} preferentially over trivalent REEs in calcite, leading to positive Eu anomalies observed in this study.

Isotope dilution measurements on nine calcite veins from the reverse faults F_{101} and F_{105} show Sm and Nd concentrations of 0.4683–3.8689 ppm and 1.0775–14.5286 ppm, respectively, and yield a Sm-Nd isochron age of 136±3 Ma (Fig. 3D), with a lower MSWD of 0.069 and an initial $^{143}Nd/^{144}Nd$ ratio of 0.512359±4. Five calcite veins from the drill cores have relatively lower Sm and Nd concentrations, ranging from 0.2044 to 0.812 ppm and 0.457 to 0.9904 ppm, respectively, and yield another Sm-Nd isochron age of 134±3 Ma (Fig. 3B), with a lower MSWD of 0.009 and an initial $^{143}Nd/^{144}Nd$ ratio of 0.511805±6. The straight lines shown in Fig. 3B and D can be interpreted in two ways, either an isochron or the result of mixing two end members with quite different $^{143}Nd/^{144}Nd$ and $^{147}Sm/^{144}Nd$ ratios (Bell et al., 1989). The absence of relationships on 1/Nd – $^{143}Nd/^{144}Nd$ diagrams for these calcites lead us to interpret the Sm-Nd data in terms of the isochron model. If such a model is accepted, then the Sm-Nd ages of these calcite veins place important constraints on the age of decarbonation and calcite veins associated with gold mineralization. Hence, the time of gold deposition in the Shuiyindong deposit would be about 135±3 Ma. This age is close to the Sm-Nd isochron ages of fluorite veins (148±9 Ma to 142±16 Ma) (Fig. 4) coeval with gold and antimony mineralization at the Qinglong deposit (Peng et al., 2003a). This fluorite is interpreted to have been formed by hydrothermal alternation of basaltic volcanic tuff during gold and antimony mineralization. These ages suggest that Au-Sb and gold mineralization in Guizhou took place during Late Jurassic to Early Cretaceous times, corresponding to the late stages of Yanshanian Orogeny (about 140 to 65 Ma), an important tectonic event in the southeastern China.

It is interesting to note that the initial ε_{Nd} values of the calcites from the reverse faults and the drill holes at 135 Ma are significantly different (−2.0 and −12.9, respectively), although they have nearly uniform $^{87}Sr/^{86}Sr$ ratios (0.707294±15, 0.707515±14, respectively) (Table 2), suggesting that Nd was derived from different sources during decarbonation and gold deposition. The relative higher initial ε_{Nd} value (−2.0) for the calcites from the reverse faults at the Shuiyindong deposit is close to those of the fluorites (−3.7 to −5.8 at 135 Ma) at the Qinglong deposit (Peng et al., 2003a), and in the range of values for Permian Maokou limestone (−6.3) and basaltic volcanic tuff (+1.5; based on the data in Peng et al., 2003a at 135 Ma). Thus, the ε_{Nd} value might be sourced from mixtures of basaltic volcanic tuff and bioclastic limestone, such as in the first unit of the Longtan Formation. The unusual concentrations of Cr (2 to 27 ppm) and Ni (13 to 17 ppm) in the calcite veins support this interpretation. The lowest initial ε_{Nd} value (−12.9) for the calcites from the drill holes is very similar to the shale of the Permian Longtan Formation (−12.7) in the southeastern China, calculating from the data of Chen and Jahn (1998) at 135 Ma. These data suggest that the Nd in the calcite veins related to decarbonation and gold deposition was most likely derived from contrasting units of the Permian Longtan Formation that hosts all ore bodies at the deposit (Fig. 1).

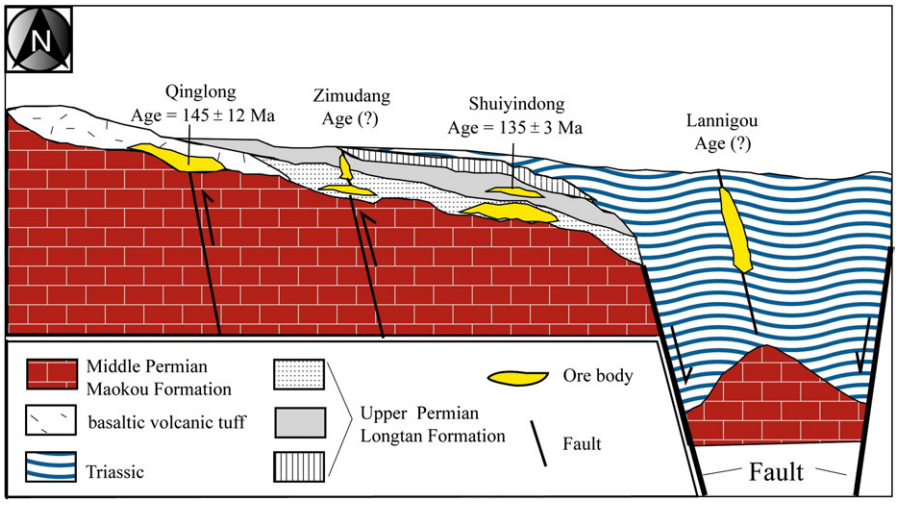

Fig. 4. Schematic cross section with the ages of Carlin-type gold deposits in Guizhou. The age of the Qinglong deposit is from Peng et al. (2003a).

5. Conclusions

This present study documents the first Sm-Nd isochron ages (134–136 Ma) on hydrothermal calcite veins associated with decarbonation and gold deposition from the Shuiyindong Carlin-type gold deposit. These ages represent the age of decarbonation that provided the main source of iron for sulfidation during gold deposition. Initial Nd isotopic compositions indicate that Nd was derived from the host limestones. The data indicates that Carlin-type gold mineralization in Guizhou took place during Late Jurassic to Early Cretaceous times, corresponding to the late stages of the Yanshanian Orogeny.

Considering that hydrothermal calcite is a common mineral in Carlin-type gold deposits, Sm-Nd dating of calcites with relative high contents of REEs and MREE-enriched patterns may be useful in the ages of other Carlin-type gold deposits.

Acknowledgements

This research was supported by the State Key Basic Research Program of China (No. 2007CB411402), the National Sciences Foundation of China (No. 40672067), and the project of the Ministry of Science and Technology of China (No. 2006BAB01A13). Dr. Xianglin Tu, Prof. Yuanxian Lin and Mrs. Hui Liu are greatly appreciated for their help with analyses and technical assistance. Editor David Rickard and an anonymous referee are thanked for their thoughtful and thorough reviews.

References

Bell, K., Anglin, C.D., Franklin, J.M., 1989. Sm-Nd and Rb-Sr isotope systematics of scheelites: possible implications for the age and genesis of vein-hosted gold deposits. Geology 17, 500–504.

Chakurian, A.M., Arehart, G.B., Donelick, R.A., Zhang, X., Reiners, P.W., 2003. Timing constraints of gold mineralization along the Carlin trend utilizing apatite fission-track, $^{40}Ar/^{39}Ar$, and apatite (U-Th)/He. Economic Geology 98, 1159–1171.

Chen, J.F., Jahn, B., 1998. Crustal evolution of southeastern China: Nd and Sr isotopic evidence. Tectonophysics 284, 101–133.

Chesley, J.T., Halliday, A.N., Scrivener, R.C., 1991. Samarium-neodymium direct dating of fluorite mineralization. Science 252, 949–951.

Darbyshire, D.P.F., Pitfield, P.E.J., Campbell, S.D.G., 1997. Late Archean and Early Proterozioc gold-tungsten mineralization in the Zimbabwe Archean craton: Rb-Sr and Sm-Nd isotope constrains. Geology 24, 19–22.

Emsbo, P., Hofstra, A.H., Lauha, E.A., Griffin, G.L., Hutchinson, R.W., 2003. Origin of high-grade gold ore, source of ore fluid components and genesis of the Meikle and neighboring Carlin-type deposits, north Carlin Trend, Nevada. Economic Geology 98, 1069–1105.

Groff, J.A., Heizler, M.T., McIntosh, W.C., Norman, D.I., 1997. $^{40}Ar/^{39}Ar$ dating and mineral paragenesis for Carlin-type gold deposits along the Getchell trend: evidence for Cretaceous and Tertiary mineralization. Economic Geology 92, 601–622.

Halliday, A.N., Shepherd, J.T., Dicken, A.P., Chesley, J.T., 1990. Sm-Nd evidence for the age and origin of a MVT ore deposit. Nature 344, 54–56.

Herrmann, A.G., 1970. Yttrium and Lanthanides. In: Wedepohl, K.H. (Ed.), Handbook of Geochemistry, vol. II/2. Springer-Verlag, Berlin, pp. 57–71. Section 39.

Hofstra, A.H., Cline, J.S., 2000. Characteristics and models for Carlin-type gold deposits. Reviews in Economic Geology 13, 163–220.

Hofstra, A.H., Leventhal, J.S., Northrop, H.R., Landis, G.P., Rye, R.O., Birak, D.J., Dahl, A.R., 1991. Genesis of sediment-hosted disseminated gold deposits by fluid mixing and sulfidization: chemical-reaction-path modeling of ore-depositional processes documented in the Jerritt Canyon District, Nevada. Geology 19, 36–40.

Hu, R.Z., Su, W.C., Bi, X.W., Tu, G.Z., Hofstra, A.H., 2002. Geology and geochemistry of Carlin-type gold deposits in China. Mineralium Deposita 37, 378–392.

Johannesson, K.H., Lyons, W.B., 1995. Rare-earth element geochemistry of Colour Lake, an acidic freshwater lake on Axel Heiberg Island, Northwest Territories, Canada. Chemical Geology 119, 209–223.

Johannesson, K.H., Lyons, W.B., Yelken, M.A., Gaudette, H.E., Stetzenbach, K.J., 1996. Geochemistry of rare-earth elements in hypersaline and dilute acidic natural terrestrial waters: complexation behaviour and middle rare-earth element enrichment. Chemical Geology 133, 124–144.

Kesler, S.E., Riciputi, L.C., Ye, Z.J., 2005. Evidence for a magmatic origin for Carlin-type gold deposits: isotopic composition of sulfur in the Betze-Post-Screamer deposit, Nevada, USA. Mineralium Deposita 40, 127–136.

Lovering, T.G., 1972. Jasperoid in the United States - its characteristics, origin, and economic significance. U.S. Geological Survey Professional Paper 710, p. 164.

Ludwig, R.K., 1996. ISOPLOT: a plotting and regression program for radiogenic-isotope data (Version 2.9). U.S. Geological Survey Open-File Report 91–445, p. 47.

Peng, J.T., Hu, R.Z., Jiang, G.H., 2003a. Samarium-neodymium isotope system of fluorites from the Qinglong antimony deposit, Guizhou Province: constraints on the mineralizing age and ore-forming minerals' sources. Acta Petrologica Sinica 19, 785–791 (in Chinese with English abstract).

Peng, J.T., Hu, R.Z., Burnard, P.G., 2003b. Samarium-neodymium isotope systematics of hydrothermal calcites from the Xikuangshan antimony deposit (Hunan, China): the potential of calcite as a geochronometer. Chemical Geology 200, 129–136.

Stenger, D.P., Kesler, S.E., Peltonen, D.R., Tapper, C.J., 1998. Deposition of gold in Carlin-type gold deposits: the role of sulfidation and decarbonation at Twin Creeks, Nevada. Economic Geology 93, 201–215.

Su, W.C., 2002. The Hydrothermal Fluid Geochemistry of the Carlin-type Gold Deposits in Southwestern Yangtze Craton, China. Unpublished Ph.D. Thesis, Guiyang, China, Institute of Geochemistry, Chinese Academy of Sciences (in Chinese with English Abstract).

Su, W.C., Xia, B., Zhang, H.T., Zhang, X.C., Hu, R.Z., 2008. Visible gold in arsenian pyrite at the Shuiyindong Carlin-type gold deposit. Guizhou, China: implications for the environment and processes of ore formation. Ore Geology Reviews 33, 667–679.

Su, W.C., Heinrich, C.A., Pettke, T., Zhang, X.C., Hu, H.R., Xia, B., in press. Sediment-hosted gold deposits in Guizhou, China: products of wallrock sulfidation by deep crustal fluids. Economic Geology.

Sverjensky, D.A., 1984. Europium redox equilibria in aqueous solution. Earth Planetary Science Letters 67 (1), 70–78.

Tretbar, D.R., Arehart, G.B., Christensen, J.N., 2000. Dating gold deposition in a Carlin-type gold deposit using Rb/Sr methods on the mineral galkhaite. Geology 28, 947–950.